Nano LDH catalyst with high CO_2 adsorption capability for photocatalytic reduction

メタデータ	言語: eng
	出版者:
	公開日: 2018-08-22
	キーワード (Ja):
	キーワード (En):
	作成者: Tokudome, Yasuaki, Fukui, Megu, Iguchi, Shoji, Hasegawa, Yudai, Teramura, Kentaro, Tanaka, Tsunehiro, Takemoto, Masanori, Katsura, Reo, Takahashi, Masahide
	メールアドレス:
	所属:
URL	http://hdl.handle.net/10466/16032

Journal Name

ARTICLE

Nano LDH catalyst with high CO$_2$ adsorption capability for photo-catalytic reduction

Yasuaki Tokudome,*[a] Megu Fukui,[a] Shoji Iguchi,[b] Yudai Hasegawa,[b] Kentaro Teramura,*[bc] Tsunehiro Tanaka,[bc] Masanori Takemoto,[a] Reo Katsura,[a] and Masahide Takahashi[a]

A benign catalyst with a considerable activity towards CO$_2$ reduction has been demanded to explore green processes. Layered double hydroxide (LDH) is a promising candidate material for this purpose, because it exhibits a high catalytic activity even in aqueous solvents, free from poisoning by water molecules. Herein, we demonstrate that NiAl LDH nanocrystals (~ 20 nm) exhibit a remarkably high photocatalytic activity toward CO$_2$ reduction in aqueous media, thanks to their capability of adsorbing CO$_2$ in high concentration. The present LDH photocatalyst with a high catalytic activity was obtained through a nanocrystallization induced by a homogenous and rapid pH increase from an aqueous solution of concentrated metal salts. The rate of photocatalytic CO$_2$ reduction over the nano LDH catalyst (50 μmol/h) is 7 times higher than that over a highly-crystalline standard LDH catalyst (7.2 μmol/h) prepared through a conventional method. Systematic investigation revealed that the excellent catalytic property of the present nano LDH is originated from its high affinity towards CO$_2$ introduced as the gaseous state. This specific nature of the surface could be related to the metastable surface which was quenched by rapid hydroxide formation from concentrated solution of metals salts. The nano LDH catalysts demonstrated here can be synthesized in a simple one-pot reaction in aqueous solvent at a mild temperature. Further exploration into material design by complexing with co-catalysts would open up catalysts for artificial photosynthesis based on nano LDH materials.

Introduction

Coupling CO$_2$ reduction and water oxidation under sunlight is a great challenge to achieve artificial photosynthesis.[1] A benign catalyst with a considerable activity towards CO$_2$ reduction has been demanded for this scheme and extensively investigated.[2, 3] Metal oxides and sulfides have been explored as photocatalysts,[2] and among them, Ga$_2$O$_3$ and MgO were demonstrated to catalyze reductive conversion of CO$_2$ with H$_2$ as a reductant.[4] On the other hand, basic sites of these materials are easily poisoned by water and their use in aqueous media is strictly limited. To date, the photocatalytic reduction of CO$_2$ in liquid water has been assuredly demonstrated for a limited number of metal oxides, such as metal tantalates,[5-7] Zn-loaded

Ga$_2$O$_3$,[8, 9] and ALa$_4$Ti$_4$O$_{15}$ (A = Ca, Sr, and Ba),[10] with reliable evidences of stoichiometric oxidation/reduction and experiment results using gaseous ^{13}CO$_2$ as a reactant.

Apart from metal oxides, recent studies have revealed that layered double hydroxides (LDHs) selectively adsorb CO$_2$ and photo-catalytically reduce it into CO in aqueous media.[11] The general formula of LDH is [M$^{2+}_{1-x}$M$^{3+}_x$(OH)$_2$][A$_{x/n}^{n-}$·mH$_2$O], where M^{2+} and M^{3+} are di- and trivalent cations, and A^{n-} is an anion. LDH was reported to exhibit a high selectivity towards the catalytic reduction of CO$_2$ against the competitive reaction of H$_2$ production via H$_2$O reduction. The availability of LDHs as photocatalysts for CO$_2$ reduction in aqueous solvents presents a clear contrast to most of complex catalysts and oxide-based catalysts requiring dried atmospheres or vacuum conditions.[12, 13] It should be underlined that hydroxides can be much smaller in size with much higher surface area compared to standard metal-oxide catalysts prepared through calcination processes. Nanometric LDH particles are especially expected to take advantage of increased surface area and selective exposure of crystal-edges that have been considered as catalytic active sites. On the other hand, platelets of standard LDH crystals rapidly grow along the lateral dimension exceeding a micron-size scale,[14] which prevents the rational design of nano morphology of LDH catalysts. Due to this critical limitation, previous studies on hydroxide-based photocatalysts for CO$_2$ reduction have relied on tuning chemical composition.[15] Developing a scheme to control morphologies (size, shape, surface), especially in nm scale, is highly demanded to achieve a higher catalytic activity and a better reaction selectivity of hydroxide-based catalysts

[a.] Department of Materials Science, Graduate School of Engineering, Osaka Prefecture University, 1-1, Gakuencyo, Naka-ku, Sakai, Osaka, 599-8531, Japan.
[b.] Department of Molecular Engineering, Graduate School of Engineering, Kyoto University, Kyotodaigaku Katsura, Nishikyo-ku, Kyoto 615-8510, Japan.
[c.] Elements Strategy Initiative for Catalysts & Batteries (ESICB), Kyoto University, 1-30 Goryo-Ohara, Nishikyo-ku, Kyoto 615-8245, Japan.
Present affiliation of S. Iguchi: Department of Chemical Science and Engineering, Tokyo Institute of Technology, 2-12-1, Ookayama, Meguro-ku, Tokyo 152-8550, Japan
* tokudome@mtr.osakafu-u.ac.jp (Y. Tokudome); teramura@moleng.kyoto-u.ac.jp (K. Teramura)

Figure 1. Schematic illustration of the synthesis and photocatalytic application of nanohydroxide. TEM image showing typical nanostructure of nano LDH prepared at Ni/Al =2 (NLDH-2 in Table S1).

based on high affinity to reactants, controlled molecular/ion diffusion, and molecular sieving.

Herein, we found that NiAl-Cl LDH nanocrystals (~ 20 nm) exhibit a remarkably high photocatalytic activity toward CO_2 reduction in aqueous media, thanks to their capability of adsorbing CO_2 in high concentration (**Figure 1**). The nanocrystallization was achieved under a high degree of supersaturation by a homogenous and rapid pH increase from an aqueous solution of concentrated metal salts.[16, 17] The rate of photocatalytic CO_2 reduction over the nano LDH catalyst (50 μmol/h) is 7 times higher than that over a highly-crystalline standard NiAl LDH catalyst (7.2 μmol/h) prepared through a conventional method. Whilst the reaction selectivity towards CO evolution is as high as 80 % for the nano LDH catalyst. The photocatalytic activity of the nano LDH catalyst is also superior to that with a ultrathin ZnAl LDH nanosheet (≤ 0.76 μmol/h (100 mg of catalyst)).[18] The origin of the excellent catalytic properties of the nano LDH was further investigated by using various types of nano LDHs with controlled morphological and crystalline natures. Systematic investigation revealed that high affinity towards CO_2 of the metastable LDH surface formed under a high degree of supersaturation is related to the excellent catalytic activity. The ease and versatility of the present synthesis of nano LDHs allows us to further explore into material design by complexing with co-catalysts for the development of catalysts taking advantage of the CO_2 adsorption characteristics of nano LDH.

Experimental Section

Chemicals.

Nickel (II) chloride hexahydrate ($NiCl_2 \cdot 6H_2O$: 98%), aluminum chloride hexahydrate ($AlCl_3 \cdot 6H_2O$: 98%), ethanol (EtOH: 99.5%), isopropyl alcohol (IPA: >99.7%), sodium hydroxide (NaOH: 97%) were purchased from Wako Pure Chemicals Industries. Propylene oxide (PO: ≥99%) and poly(ethylene oxide) (PEO: Mv = 1.0×10^6) were purchased from Sigma-Aldrich Co. All the chemicals were used as received.

Synthesis of NiAl LDH with controllable nanostructure.

Synthesis of NiAl LDH xerogels: The compositions of samples are summarized in **Table S1**. $NiCl_2 \cdot 6H_2O$ and $AlCl_3 \cdot 6H_2O$ were

dissolved in a mixture of EtOH (3 mL, 51.4 mmol) and ultrapure water (4 mL, 222 mmol)(18.2 MΩ·cm). Propylene oxide (PO) was added to the mixture at 25 °C and further stirred for 1 min to yield a homogenous solution. Then, stirring was stopped, and the mixture was transferred to a polystyrene container which had been pre-heated at 40 °C, sealed, and kept at 40 °C. After aging for 24 h at 40 °C, wet gels were submerged in 50 mL of isopropyl alcohol (IPA) and kept for > 1 h at 40 °C to exchange the liquid in pores with IPA. This solvent exchange process was repeated 8 times with fresh IPA at 40 °C to completely remove remnants of precursors and by-products produced from PO. Then, the wet gels were collected and dried at 40 °C for > 72 h. The present synthesis of the wet gel performed in a closed container from highly acidic starting solution can avoid the inclusion of atmospheric CO_2 into the system, providing LDH with Cl^- intercalated (NiAl-Cl type LDH). The synthesis of reference LDH was performed by a conventional co-precipitation method (See **Supporting Information**).

Aging process: some of the wet gels after the process of solvent exchange were stirred in NaOH aq. solution with various concentrations (1.0×10^{-4} M - 5.0 M) to induce crystal growth of LDH for 48 h. Thus obtained materials were then centrifuged, washed with water 5 times, and dried at 40 °C in air. The sample before and after NaOH treatments possess monolithic and powder shapes, respectively.

Characterization.

A field emission scanning electron microscope (FE-SEM; S-4800, Hitachi, with a thin Pt/Pd coating) and transmission electron microscopes (TEM; JEM-2000FX, JEOL, Japan and Hitachi 7650, Hitachi, Japan) were employed to observe fine structures. Crystalline nature of the film was identified by X-ray diffraction Multiflex, Rigaku) using CuKα radiation (λ = 0.154 nm). The micro/mesopore characteristics of the samples were analyzed by N_2 sorption measurements (Belsorp-mini II, Bel Japan Inc., Japan). Prior to N_2 sorption measurements, samples were heat-treated at 500 °C in air, and then outgassed under vacuum at 200 °C. Specific surface area, S_{BET}, of samples were estimated by the Brunauer-Emmett-Teller (BET) method. Inductively coupled plasma (ICP: ICPS-8000, Shimadzu Corp.) emission spectroscopy was employed to analyze the chemical composition of the samples before and after the catalytic test. Thermal programmed desorption (TPD: TPD-1-AT, Bel Japan Inc., Japan)
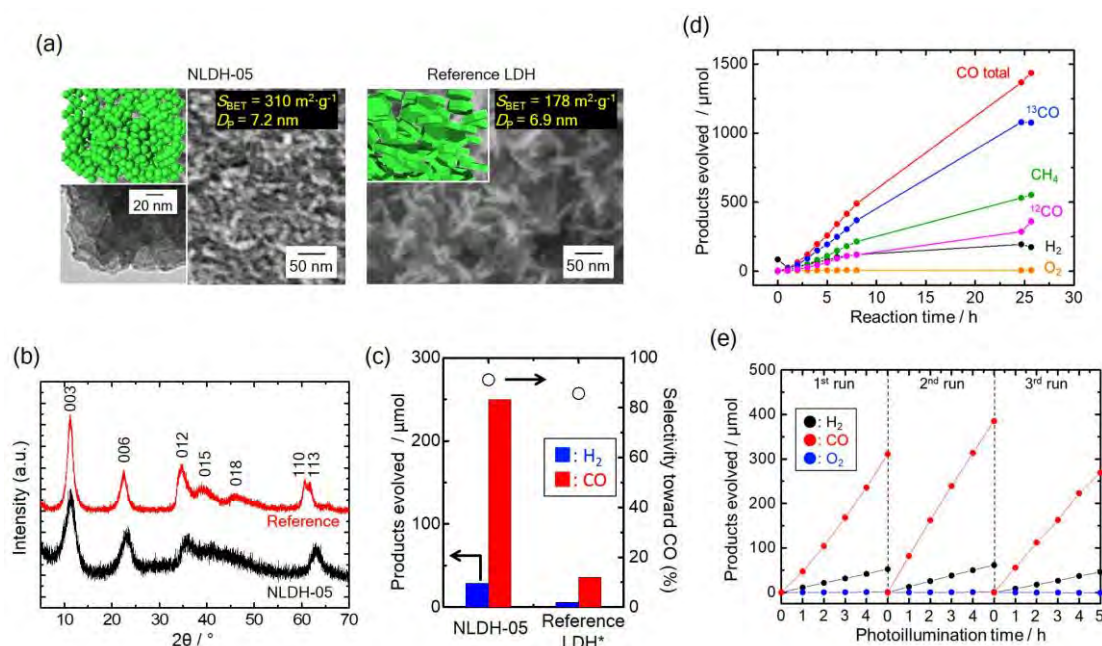
Figure 2. (a) Morphological features and (b) XRD patterns of NLDH-05 and referential LDH. S_{BET}: BET surface area; D_p: mesopore diameter. (c) Amounts of gaseous products evolved after 5 h light illumination over the LDH catalysts. *: The values from the literature (PCCP, 2015, 17, 17995). (d) Amounts of gaseous products evolved by the photocatalytic reduction of $^{13}CO_2$ over NLDH-05 catalyst. (e) Cycle characteristics of catalytic property of NLDH-05. Amounts of products as a function of photoillumination time are plotted for 3 different cycles (5 h reaction each) with intervals (> 10 h each) .

of CO_2 was used to investigate the affinity of NiAl LDH catalysts to CO_2. 50 mg of LDH sample was placed in a glass tube. After degassing the sample tube at 40 °C, CO_2 was introduced in the gas phase and allowed to adsorb on the sample surface at 40 °C for 30 min. TPD of CO_2 was measured with a ramp rate of 5 °C/min under Ar flow in the temperature range from 313 K to 1223 K. UV-vis diffusion reflectance spectra of NiAl LDH samples were measured by a UV-Visible spectrometer (V-670, JASCO, Japan) equipped with an integrating sphere. The energy gap of photo-generated electron and photo-generated hole was estimated by the Davis-Mott equation using the Kubelka-Munk function according to the previous study.[19]

Catalytic studies.

Photocatalytic CO_2 conversion was tested according to the procedure reported in our previous study.[15] **Continuous-flow system:** 1.0 g of granular LDH photocatalyst (50 mesh) was dispersed under stirring in 1.0 L of 0.1 M NaCl solution in a quartz glass reactor. CO_2 was continuously-flowed through the system at a rate of 100 mL·min^{-1} for degasification. After checking the complete degasification by GC, the flowing rate of CO_2 was set at 15 mL·min^{-1}, and the suspension was illuminated with a 400 W high pressure Hg lamp (HL400BH-9, Sen Lights Corp,, Japan) placed at the centre of the quartz glass reactor. Cooling water was circulated around the Hg lamp such that the temperature of the reaction liquid was kept at 35 °C. The gaseous products were analysed by barrier discharge ionization detector gas chromatography (BID-GC) (GC-2010 Tracera, Shimadzu Corp.). The evolution of CH_4 is considered to be derived from the decomposition of organic impurities. The

selectivity of photocatalytic reduction over LDH towards CO evolution was calculated with the following equation:

$$\text{selectivity towards CO (\%)} = 100 \times \frac{CO/\mu mol}{CO/\mu mol + H_2/\mu mol}$$

The catalytic activity was also tested using a closed circulating system with $^{13}CO_2$. The details are given in **Supporting Information**.

Results and Discussion

Nano LDH materials were prepared from an aqueous solution of high concentrations of metal salts (2.0 mol/L) through a homogenous alkalization reaction triggered by propylene oxide. The compositions of the samples are listed in **Table S1**. Starting from an acidic precursory solution containing metal chlorides, PO increases pH of the reaction mixture as a function of time. The alkalization is induced by protonation and subsequent ring-opening reaction of PO.[20] The use of propylene oxide as an alkalization reagent allows us to mix all the precursors homogenously at high concentrations and simultaneously achieve a high degree of supersaturation to crystallize nanometric metal hydroxides comprising a homogenous monolithic gel. The nanocrystalline monolithic gel possesses mesoporosity and high surface area (> 300 m^2/g) accessible by gaseous substances as confirmed by N_2 sorption. These features are advantageous to the photocatalytic application of the present nano LDH materials towards the reduction of CO_2 in water. Also, the crystallization under a high degree of

supersaturation contributes to form metastable materials in some cases; defective sites which potentially work as active sites of the catalytic reaction can be introduced in nano metal hydroxides.[21] Morphological features and catalytic activities of nano LDH samples were systematically compared with those of reference LDH prepared via a standard co-precipitation method. Reference LDH was prepared from an aqueous solution of low concentration of metal salts (0.13 mol/L) (details of the synthesis procedure is described in **Supporting Information**).[22]

Figure 2a shows morphological features of NLDH-05 and reference LDH. SEM and TEM observations confirm that NLDH-05 possesses an agglomerated nanostructure composed of nano particles with a size of 20 nm. Whilst, reference LDH are crystal platelets with various sizes ranging from 40 to 200 nm. The difference of the crystallinity is also confirmed by XRD measurement (**Figure 2b**). Diffraction peaks on the XRD pattern of NLDH-05 are broader than those of reference LDH. Crystallite sizes estimated from 003 diffraction line with Scherrer's equation are 3.44 and 5.48 nm for NLDH-05 and reference LDH, respectively. The relatively low crystallinity of NLDH-05 corresponds to the crystallization under higher degree of supersaturation; the concentration of precursory metal salts is 15 times higher in the case for NLDH-05 compared to for reference LDH. Homogenous distribution of constituent cations was confirmed by SEM-EDS mapping for both samples (**Figure S1**). **Figure 2c** shows the photocatalytic properties of LDH catalysts towards the reduction of CO_2 into CO in water. Surprisingly, NLHD-05 catalyst exhibits considerably superior CO generation (250 µmol) compared to reference LDH (36 µmol) by the photoillumination for 5h. The enhancement of 7 times of catalytic activity cannot be simply explained by the difference of the specific surface area; BET surface area, S_{BET}, = 310 and 178 m^2/g for NLDH-05 and reference LDH, respectively. The photocatalytic activity of NLDH-05 was assessed by using ^{13}C-labeled CO_2 as a CO_2 source (**Figure 2d**). The evolution of ^{13}CO was qualitatively determined at m/z = 29 on mass spectra with a calibration curve.[11] The evolution of CH_4 in the present case is considered to be derived the decomposition of organic impurities. The result revealed that 75% of total CO was indeed evolved by the reduction of $^{13}CO_2$ introduced as the gaseous state. Side reactions evolving ^{12}CO, *i.e.*, the reduction of pre-adsorbed CO_2 and the decomposition of organic impurities, were confirmed to be less significant compared to the targeted reaction in the present case. It should be emphasized that the catalytic activity maintained even after the longer reaction time of 24 h. The high durability of the nano LDH catalyst was also confirmed by repetitive catalytic reactions (**Figure 2e**). The rate of CO evolution (µmol/h) was almost constant irrespective of reaction cycles, which is in contrast with the degradative nature of standard LDH.[22] Standard NiAl LDH changed its color from green to grey during the photocatalytic reaction, implying change of valence state of Ni(II)/Ni(0) and thereby degradation of catalytic activity. Whist present nano NiAl LDH catalyst keep the original green color even after the longer reaction (cycles), where photo-generated electrons are expectedly consumed for the reduction of CO_2 at a proper rate. These results clearly demonstrate that the present nano LDH catalyst exhibit

excellent catalytic activity and selectivity toward the reduction of CO_2 in aqueous media.

A previous research reported that an artificial photosynthesis system catalyzed by LDH could be constructed by the addition of Cl^- as a hole scavenger,[22] where the overall photocatalytic reaction was experimentally confirmed to proceed as follows:

$$CO_2 + 2H^+ + 2e^- \rightarrow CO + H_2O \qquad (1)$$
$$2Cl^- + 2h^+ + H_2O \rightarrow HClO + HCl \qquad (2)$$
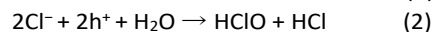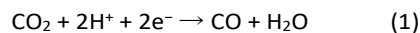
The addition of Cl^- was found to be mandatory also in the present case of using nano LDH as a catalyst (**Figure S2**), suggesting photo-generated holes are consumed by Cl^- as is the case of standard LDH catalyst. However, the generation of HClO was not confirmed by (*N,N*-dimethyl-*p*-phenylenediamine) (DPD) test[22] for the case using nano LDH as a catalyst. A possible explanation is that a series of disproportionation reactions of ClO^- yielded ClO_4^- with a high stability and less oxidative.

NiAl double hydroxides exhibit higher CO evolution with higher selectivity compared to single hydroxides of $Al(OH)_3$ and $Ni(OH)_2$ as shown in **Figure S3**. The adsorption of CO_2 on the basic surface of LDH is reportedly a key to explain the occurrence of photocatalytic reduction of CO_2 over LDH in aqueous media;[19] negligible CO_2 reduction occurs on acidic or inert oxide surfaces, such as Nb_2O_5, TiO_2, and V_2O_5 in the presence of water.[4] Regardless of starting Ni/Al ratio (Ni/Al = 0.5, 2, 4, 8), nano LDHs prepared in the present study exhibit much higher photocatalytic activity (> 180 µmol) than reference LDH (36 µmol) after the reaction for 5 h. The result implies that factors other than chemical composition play critical roles for the enhancement of the photocatalytic activity of the nano LDH towards CO_2 reduction.

Figure 3a shows the curves of CO_2 temperature-programed desorption (CO_2-TPD) for NLDH-2 with and without preliminary adsorption of CO_2 before the programed increase of temperature. The peaks at 308 °C, 457 °C, and 600 °C, are resulted from the series of deintercalation processes of CO_3^{2-} accompanied with the thermal decomposition of LDH crystals (**Figure S4**). Whilst the peak at 85 °C, which is observed only for the sample with preliminary adsorption of CO_2, can be successfully assigned to the evolution of CO_2 which had been adsorbed on the surface of LDH crystal. The peak derived from the adsorbed CO_2 at 85 °C was not clearly observed for the TPD curve of reference LDH showing a lower CO evolution of 36 µmol for 5 h (not shown). These results propose the possibility that the surface of the present nano LDH exhibits high affinity towards CO_2 to lead to the drastic improvement of photocatalytic activity. In order to verify this hypothesis, we systematically investigated other possible contributions from morphological and crystalline properties of the nano LDHs, towards the reduction of CO_2 in aqueous media. Surface area, crystallinity, and surface nature of nano LDH were independently tuned by changing starting compositions and applying post treatments. These results are closely discussed in the following sections.

As is expected, the present photocatalytic activity was independent of the introduction of large macroporosity in µm
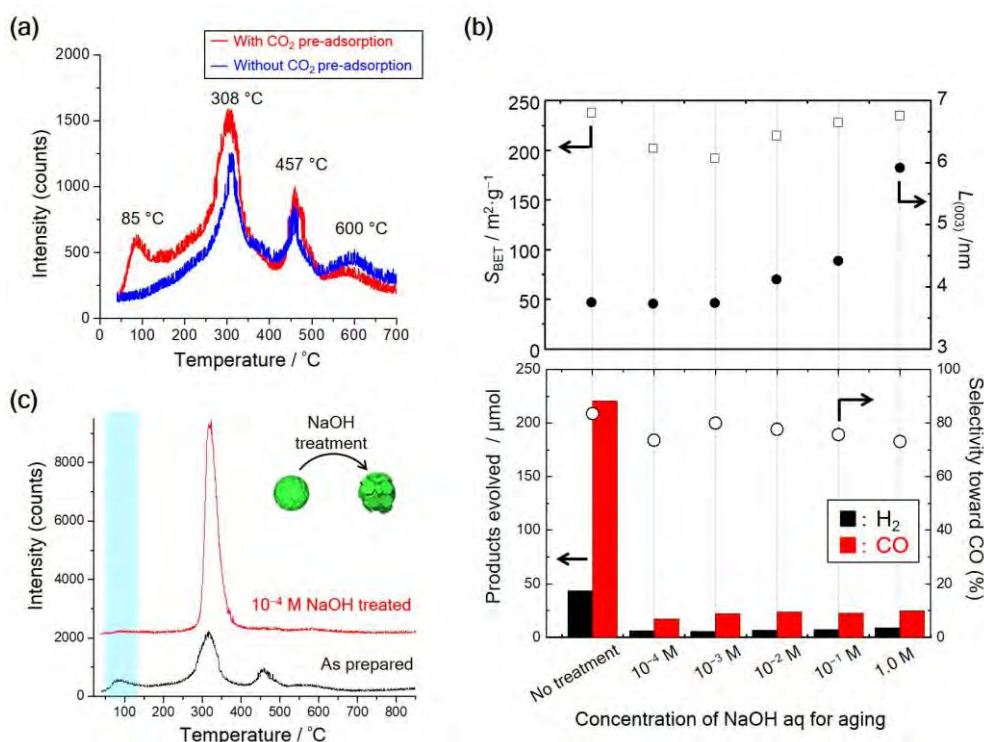
Figure 3. (a) CO_2-TPD curves of NLDH-2 with and without preliminary adsorption of CO_2. (b) Amounts of gaseous products and reaction selectivity for the reduction of CO_2 over NLDH-2 after various post treatments. The catalytic reaction was performed for 5 h. BET surface area, S_{BET}, and 003 crystallite size, $L_{(003)}$, for NLDH-2 after various aging treatments. (c) CO_2-TPD curves of NLDH-2 before and after 10^{-4} M NaOH treatment.

range because the reactant, CO_2, is a small gaseous molecule (**Figure S5**). We hereafter focus on the nano morphological features and crystallinity of the LDH catalysts. **Figure S6** shows catalytic activities of nano LDHs with different specific surface area. The results suggest that catalytic activity is not related to specific surface area of the catalysts. More clearly, CO evolution in 5 h of LDH-2-05 (246 µmol) with a relatively low surface area, S_{BET} = 93 m^2/g is superior to that of reference LDH (36 µmol) with larger surface area, S_{BET} = 178 m^2/g.

Photocatalytic property generally depends on the efficiency of charge separation as well as the size of surface area which allows large adsorption capacity of reagents.[23, 24] Indeed, calcination for oxide-based catalysts has been optimized to achieve the best balance between good crystallinity and high surface area.[25-27] The crystallinity of the hydroxide-based materials is also expected to influence on the catalytic activities. In this context, an aging process with NaOH aqueous solutions was applied to tune crystallinity of the nano LDH catalysts through a controlled dissolution-reprecipitation. Aging NLDH-2 in NaOH solutions controllably increased the crystallinity of the nano LDH (**Figure S7**). **Figure 3b** shows the summary of (003) crystallite size, $L_{(003)}$, S_{BET}, and catalytic properties of NLDH-2 after various aging treatments. The value of $L_{(003)}$ increases with NaOH concentration, suggesting the progress of dissolution-recrystallization process. S_{BET} was almost constant irrespective of the NaOH treatment; decrease of the surface area by coarsening crystallites might be compensated by the smaller shrinkage during drying for the NaOH-treated samples with a relatively high toughness.[28]

Unexpectedly, the catalytic activity considerably degrades by the treatment with NaOH in spite of the improvement of the crystallinity. Even the NaOH treatment at 10^{-4} M considerably degraded the original photocatalytic activity of NLDH-2 (220 µmol) into 17 µmol which is lower than that of standard LDH (36 µmol). On the other hand, there is no clear difference observed on the XRD patterns (**Figure S7**), 003 crystallite sizes (**Figure 3b**), and SEM-EDS mappings (**Figure S8**) for NLDH-2 before and after the treatment with 10^{-4} M NaOH. The intactness of the crystallinity is also supported by the results of UV-vis spectroscopy. The energy gaps of photo-generated electrons and photo-generated holes, E_g.[19] are comparable for NLDH-2 before and after the treatment with 10^{-4} M NaOH (**Figure S9**). These discussions clearly demonstrate that crystallinity (crystallite size and preferential exposure of the crystal-edges) and surface area of the present nano LDH catalyst do not account for the improvement of catalytic activity of 7 times.

We assessed the surface natures of the set of these nano LDHs with the same morphological features and crystallinities, and with completely different catalytic activities. **Figure 3c** shows the curves of CO_2-TPD for NLDH-2 before and after 10^{-4} M NaOH treatment. As evidenced in **Figure 3a**, the peak at 85 °C is originated from the evolution of adsorbed CO_2 on the surface of LDH crystal. The TPD curve of pristine NLDH-2 shows the peak at 85 °C, whilst that after the treatment with NaOH of 10^{-4} M does not (**Figure 3c**). These results confirm: 1) nano LDH prepared in this study exhibits a high affinity with CO_2 introduced as the gaseous state, and 2) this high affinity is degraded by the NaOH treatment. The change in the surface

nature by the NaOH treatment can be explained by the relaxation of a metastable poorly-crystalline surface into a thermodynamically-stable crystalline surface. The rapid hydrolysis of metal cations induced by PO under a high degree of supersaturation reportedly introduces defective poorly-crystallize hydroxide,[21] where defective penta-coordinated Al(III) species were introduced in the case of aluminum hydroxide. The treatment with NaOH is expected to work as a ripening process to form a thermodynamically-stable surface via a dissolution-reprecipitation. Indeed, the NLDH-2 after the treatment with 10^{-4} M NaOH shows higher stability against the process of Ni^{2+} leaching under an acidic condition (**Table S3**). It is well known that surface nature is an important parameter to tune the distribution of catalytically-active sites and to design efficient heterogeneous catalysis.[29, 30] Using an anisotropic layered crystal has been considered to be advantageous in this sense thanks to effective separation of reaction sites of reduction from those of oxidation.[10] On the contrary, the results demonstrated here shed light on another concept to improve the catalytic activity of a double hydroxide, based on the formation of metastable surface through nanocrystallization under the highly supersaturated condition. Further understanding on the adsorption mechanism of CO_2 on LDHs in a systematic manner is a future topic of interests to develop LDH-based photocatalysts.

Conclusions

Nano LDH prepared under a high degree of supersaturation has been found to exhibit a high photocatalytic activity towards reduction of CO_2 in water. The rate of CO evolution (50 µmol/h) was 7 times higher than that of standard LDH (7.2 µmol/h). Whilst the reaction selectivity towards CO evolution is as high as 80 % for the nano LDH catalyst. Systematic investigation revealed that the excellent catalytic property of the present nano LDH is originated from its high affinity towards CO_2 introduced as the gaseous state. This specific nature of the surface would be related to the metastable surface which was quenched by rapid hydroxide formation with propylene oxide from concentrated solution of metals salts. The nano LDH catalysts demonstrated here can be synthesized in a simple one-pot reaction in aqueous solvent at a mild temperature. Moreover, the chemical tuning and the nanostructuration are allowed by simply changing the synthesis conditions. Further exploration into material design by complexing with co-catalysts would open up catalysts for artificial photosynthesis based on nano LDH materials.

Conflicts of interest

The authors declare that they have no conflict of interest.

Acknowledgements

Notes and references

1.   W. Kim, B. A. McClure, E. Edri and H. Frei, *Chem. Soc. Rev.*, 2016, **45**, 3221-3243.
2.   S. Navalón, A. Dhakshinamoorthy, M. Álvaro and H. Garcia, *ChemSusChem*, 2013, **6**, 562-577.
3.   W. Tu, Y. Zhou and Z. Zou, *Adv. Mater.*, 2014, **26**, 4607-4626.
4.   H. Tsuneoka, K. Teramura, T. Shishido and T. Tanaka, *J. Phys. Chem. C*, 2010, **114**, 8892-8898.
5.   S. Iguchi, K. Teramura, S. Hosokawa and T. Tanaka, *Catal. Sci. Technol.*, 2016, **6**, 4978-4985.
6.   T. Takayama, H. Nakanishi, M. Matsui, A. Iwase and A. Kudo, *J. Photochem. Photobiol. A*, 2017, DOI: 10.1016/j.jphotochem.2017.10.002.
7.   H. Nakanishi, K. Iizuka, T. Takayama, A. Iwase and A. Kudo, *ChemSusChem*, 2017, **10**, 112-118.
8.   K. Teramura, Z. Wang, S. Hosokawa, Y. Sakata and T. Tanaka, *Chem. - Eur. J.*, 2014, **20**, 9906-9909.
9.   Z. Wang, K. Teramura, Z. Huang, S. Hosokawa, Y. Sakata and T. Tanaka, *Catal. Sci. Technol.*, 2016, **6**, 1025-1032.
10.   K. Iizuka, T. Wato, Y. Miseki, K. Saito and A. Kudo, *J. Am. Chem. Soc.*, 2011, **133**, 20863-20868.
11.   K. Teramura, S. Iguchi, Y. Mizuno, T. Shishido and T. Tanaka, *Angew. Chem. Int. Ed.*, 2012, **51**, 8008-8011.
12.   J. L. White, M. F. Baruch, J. E. Pander Iii, Y. Hu, I. C. Fortmeyer, J. E. Park, T. Zhang, K. Liao, J. Gu, Y. Yan, T. W. Shaw, E. Abelev and A. B. Bocarsly, *Chem. Rev.*, 2015, **115**, 12888-12935.
13.   D. Wang, R. Huang, W. Liu, D. Sun and Z. Li, *ACS Catal.*, 2014, **4**, 4254-4260.
14.   G. J. A. A. Soler-Illia, Jobbágy M., Regazzoni, A. E., Blesa, M. A. , *Chem. Mater.*, 1999, **11**, 3140-3146.
15.   S. Iguchi, K. Teramura, S. Hosokawa and T. Tanaka, *Catal. Today*, 2015, **251**, 140-144.
16.   Y. Tokudome, K. Fujita, K. Nakanishi, K. Miura and K. Hirao, *Chem. Mater.*, 2007, **19**, 3393-3398.
17.   Y. Tokudome, N. Tarutani, K. Nakanishi and M. Takahashi, *J. Mater. Chem. A*, 2013, **1**, 7702-7708.
18.   Y. Zhao, G. Chen, T. Bian, C. Zhou, G. I. N. Waterhouse, L. Z. Wu, C. H. Tung, L. J. Smith, D. O'Hare and T. Zhang, *Adv. Mater.*, 2015, **27**, 7824-7831.
19.   S. Iguchi, S. Kikkawa, K. Teramura, S. Hosokawa and T. Tanaka, *PCCP*, 2016, **18**, 13811-13819.
20.   A. E. Gash, T. M. Tillotson, J. H. Satcher, J. F. Poco, L. W. Hrubesh and R. L. Simpson, *Chem. Mater.*, 2001, **13**, 999-1007.
21.   Y. Tokudome, *J. Ceram. Soc. Jpn.*, 2017, **125**, 597-602.
22.   S. Iguchi, K. Teramura, S. Hosokawa and T. Tanaka, *PCCP*, 2015, **17**, 17995-18003.
23.   A. Kudo and Y. Miseki, *Chem. Soc. Rev.*, 2009, **38**, 253-278.

24. S. K. Choi, S. Kim, S. K. Lim and H. Park, *J. Phys. Chem. C*, 2010, **114**, 16475-16480.
25. K. Ikarashi, J. Sato, H. Kobayashi, N. Saito, H. Nishiyama and Y. Inoue, *J. Phys. Chem. B*, 2002, **106**, 9048-9053.
26. Z. Wang, K. Teramura, S. Hosokawa and T. Tanaka, *J. Mater. Chem. A*, 2015, **3**, 11313-11319.
27. T. Guohui, F. Honggang, J. Liqiang, X. Baifu and P. Kai, *J. Phys. Chem. C*, 2008, **112**, 3083-3089.
28. Y. Tokudome, K. Nakanishi, K. Kanamori, K. Fujita, H. Akamatsu and T. Hanada, *J. Colloid Interface Sci.*, 2009, **338**, 506-513.
29. T. F. Jaramillo, K. P. Jorgensen, J. Bonde, J. H. Nielsen, S. Horch and I. Chorkendorff, *Science*, 2007, **317**, 100-102.
30. R. Narayanan and M. A. El-Sayed, *J. Phys. Chem. B*, 2005, **109**, 12663-12676.

Supporting Information

Nano LDH catalyst with high CO₂ adsorption capability for photocatalytic reduction

Yasuaki Tokudome, Megu Fukui, Shoji Iguchi, Yudai Hasegawa, Kentaro Teramura,
Tsunehiro Tanaka, Masanori Takemoto, Reo Katsura, Masahide Takahashi

Supporting Notes

Supporting Table

Supporting Figures

Supporting Notes:

Synthesis of reference LDH

The synthesis was performed according to the procedure described in a previous report.[1] $NiCl_2 \cdot 6H_2O$ (32 mmol) and $AlCl_3 \cdot 6H_2O$ (8.0 mmol) were dissolved in 100 mL of ultrapure water. This salt solution was added dropwise into 200 mL of Na_2CO_3 aqueous solution (0.025 mol/L) under stirring at a room temperature. During the hydrolysis of the salt solution, pH was monitored and 0.2 mol/L of NaOH aq. was added to keep the solution pH = 10. The mixture was then aged for 1.5 h at a room temperature to yield sedimentation. The sedimentation was placed in a teflon-lined closed vessel and reacted at 110 °C for 20 h. Thus obtained crystals were filtrated and washed with ultrapure water three times and dried at 110 °C for 3 days. The sample is obtained as $NiAl-CO_3$ type LDH.

Catalytic studies. *closed circulating system with 13-labeded CO_2 ($^{13}CO_2$):* NLDH-05 was prepared in the presence of 0.03 g poly(ethylene) oxide ($M_v = 1.0 \times 10^6$) according to the procedure described in Experimental section of the main text. 0.8 g of granular LDH photocatalyst (25 mesh) was dispersed under stirring in 350 mL of 0.1 M NaCl solution in a quartz glass reactor. The reactor containing the suspension was degassed under reduced pressure. CO_2 purified by vacuum distillation at liquid nitrogen temperature was introduced into the free gas space of the system, and the circulating was performed for 1 h before photoillumination. Then, the suspension was illuminated with a 400 W high pressure Hg lamp (HL400BH-9, Sen Lights Corp,, Japan) placed at the center of the quartz glass reactor. Cooling water was circulated around the Hg lamp. The gaseous products were analyzed by thermal conductivity detector gas chromatography (TCD-GC) using a GC-8A chromatograph (Shimadzu Corporation, Japan) equipped with a MS-5A packed column. A quadruple-type mass spectrometer (MS: BEL Mass, BEL Japan, Inc.) was used distinguish ^{12}CO and ^{13}CO for the isotope experiment using $^{13}CO_2$. Total amount of evolved CO was measured with TCD-GC, and ^{13}CO was quantitatively determined with MS at m/z = 29 with a calibration curve. ^{12}CO was calculated as a difference as total amount of CO and ^{13}CO. The closed circulating system was used for the catalytic study with 13-labeded CO_2 ($^{13}CO_2$) (**Figure 2d**). Other catalytic experiments were performed with a continuous-flow system.

Note that The difference of intercalating anions between NLDH and reference LDH does not matter in the catalytic tests in the present study because CO_2 bubbling for the catalytic reaction replace Cl^- with CO_3^{2-} to form $NiAl-CO_3$ type LDH at the beginning of the reaction for all the samples.

Supporting Tables:

Table S1. Starting compositions of the prepared LDH photocatalysts.

ID	Ni/Al	PO/ (M(III)+M(II))	AlCl$_3$·6H$_2$O /g	NiCl$_2$·6H$_2$O /g	PO /mL
NLDH-05	0.5	2.8	1.90	0.93	2.27
NLDH-2	2	2.8	0.95	1.86	2.27
NLDH-4	4	2.8	0.57	2.23	2.27
NLDH-8	8	2.8	0.32	2.48	2.27
Al(OH)$_3$	0	2.8	2.85	-	2.27
Ni(OH)$_2$	∞	2.8	-	2.79	2.27

Note: the amount of solvent was set at constant; a mixture of EtOH (3 mL, 51.4 mmol) and H$_2$O (4 mL, 222 mmol). The NiAl hydrogel with hierarchical porous structure was prepared by adding 0.03 g of poly(ethylene oxide) (PEO) to the starting metal salt solution.

Table S2. Composition of samples appeared on Figure S5.

| ID	Ni/Al	PO / (M(II) + M(III))	Relative concentration of metal salts	AlCl$_3$· 6H$_2$O /g	NiCl$_2$· 6H$_2$O /g	PO /mL
NLDH-2-2	2	2.8	**2**	1.90	3.72	4.54
NLDH-2	2	2.8	**1**	0.95	1.86	2.27
NLDH-2-05	2	2.8	**0.5**	0.48	0.93	1.14

Note: The amount of solvent was set at constant; a mixture of EtOH (3 mL, 51.4 mmol) and H$_2$O (4 mL, 222 mmol).

Table S3. Summary of ICP analyses on LDH catalysts before and after exposure to an acidic condition. Pristine LDH and NaOH-treated LDH were exposed to an acidic condition. ICP measurement was performed on these samples before and after the acidic treatment. The NaOH-treated LDH after exposure to an acidic condition shows relatively higher Ni/Al ratio (Ni/Al = 1.36) compared to pristine LDH after the exposure to the same acidic condition (Ni/Al =1.08). Under a weakly acidic condition, Ni^{2+} tends to leach out from the NiAl double hydroxide material to form a solid with a relatively lower Ni/Al ratio; the solubility products, K_{sp}, of $Al(OH)_3$ and $Ni(OH)_2$ are $10^{-32.4}$ and $10^{-14.5}$, respectively. Therefore, these results confirm that LDH treated with NaOH exhibits relatively high chemical stability under the acidic condition.

aging applied	*Catalytic activity*	*Ni/Al (ICP)*	
		As prepared	After exposure to an acidic condition*
Pristine (No treatment)	High (44 μmol/h)	1.99	1.08
10^{-4} M NaOH	Low (3.4 μmol/h)	1.95	1.36

*1.0 g of sample was suspended in 0.1 M NaCl solution into which CO_2 was continuously introduced in the gas phase for 5 h.

Supporting Figures:
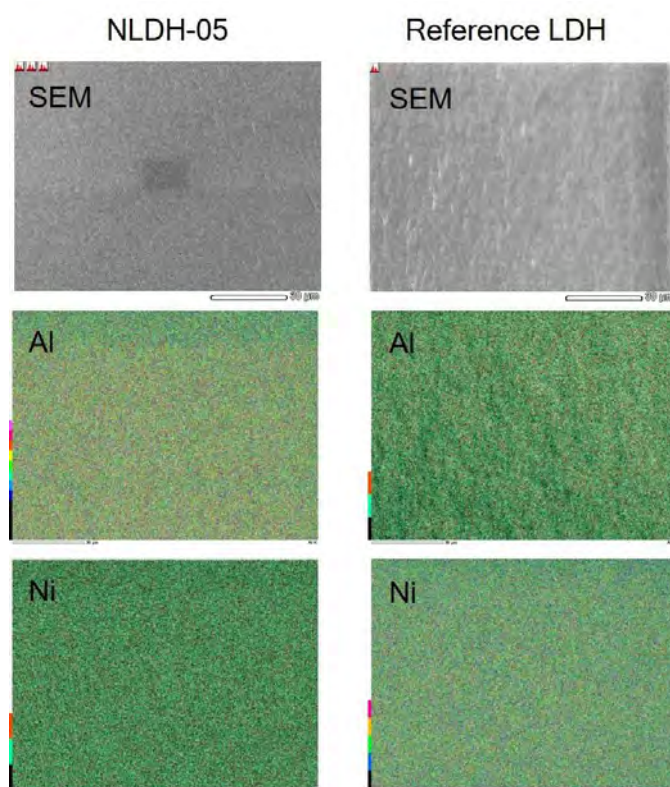
Figure S1. Elemental mappings of NLDH-05 and reference LDH. Both photocatalysts show homogeneous distribution of constituent cationic species (Ni(II) and Al(III)). A scanning electron microscope with an energy-dispersive X-ray spectrometer (SEM-EDS, JSM-6060S, JEOL) was used for the analysis.
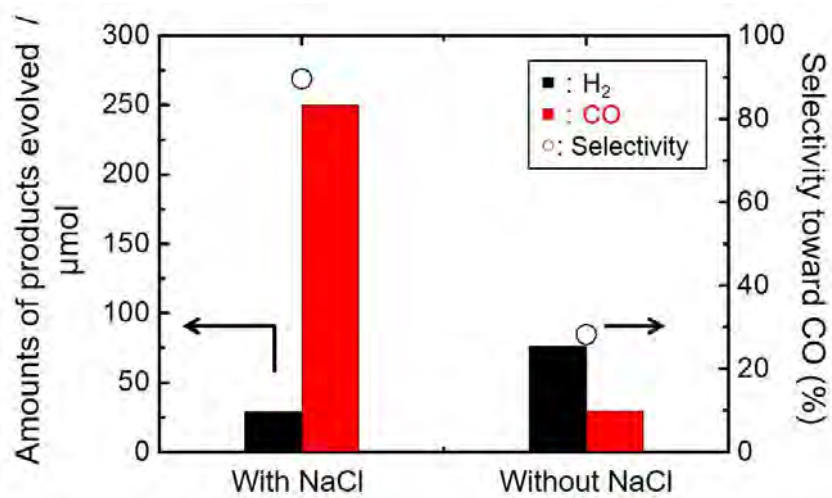
Figure S2. Amounts of gaseous products evolved after the photocatalytic reduction of CO_2 with and without NaCl additive. The reaction time: 5 h. Sample: NLDH-05.
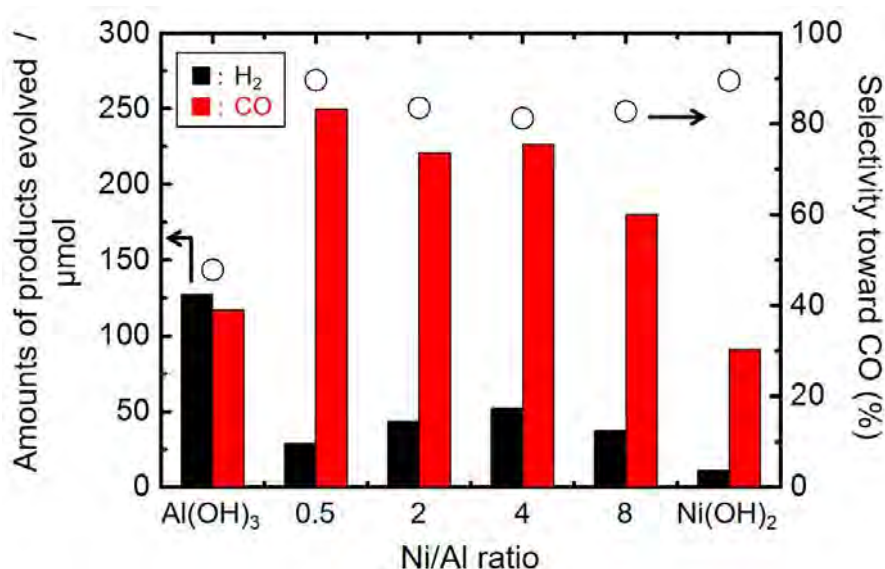
Figure S3. Amounts of gaseous products and reaction selectivity for the photocatalytic CO_2 reduction over LDH catalysts prepared with various compositions (Ni/Al ratio). Photoillumination: 5 h. The starting compositions of the samples are listed in **Table S1**.

The selectivity of photocatalytic CO_2 reduction over LDH catalysts were reported to depend on (or independent of) the following factors:

1) The choice of anionic species which work as a hole scavenger influences on the selectivity. Chloride anion, employed in the present study, is reported to be the best hole scavenger in terms of selectivity (there is negligible effect on selectivity of counter cation introduced as a metal chloride). [1]

2) The selectivity considerably depends on the types of M(II) and M(III) involved in the double hydroxide; for example Ni(II)/Al(III) shows much higher selectivity toward CO_2 compared to Mg(II)/Al(III).[2]

3) The selectivity for the standard LDH does not depend on the Ni/Al ratio and almost constant for NiAl LDH with compositions in the range of Ni/Al = 2-5.[1]

Photocatalysts discussed in the present manuscript are NiAl-type LDH with a Ni/Al ratio between 0.5-8. The reaction was performed in 0.1 M NaCl aq.

It should be highlighted that the present study successfully reveals that the size of the crystals, crystallinity, surface nature (metastability) also does not influence on the reaction selectivity.
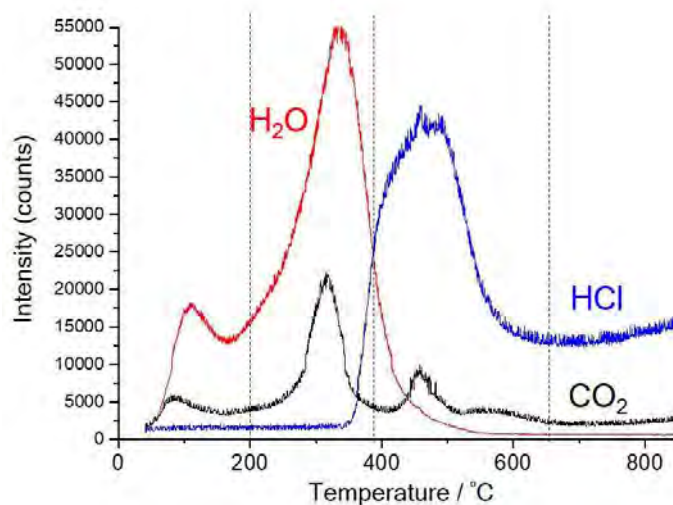
Figure S4. TPD curves of H_2O (red), HCl (blue), and CO_2 (back) measured for NLDH-2. The destruction of hydroxide crystals is reportedly accompanied with the evolution of H_2O and charge-compensating anions and/or chelating anions as a gaseous species.[3] NLDH-2 mainly contains Cl^- as an intercalating anion, whereas atmospheric CO_2 gradually replace Cl^- as CO^{2-} during the solvent exchange process with IPA, and subsequent drying process. Considering possible thermal events for LDH crystals, the CO_2 TPD curve (black) in **Figure S3** can be interpreted as follows; the evolution of CO_2 appeared as a peak at 308 °C, which is accompanied with the evolution of H_2O, is originated from the deintercalation of CO_3^{2-} by the dehydration of hydroxide sheets of LDH. The evolution of CO_2 appeared as broad peaks at 457 and 600 °C, which is accompanied with HCl evolution, can be explained by the complete desorption of CO_3^{2-} upon crystallization of the dehydrate oxide into crystalline phases ($NiAl_2O_4$ and NiO).
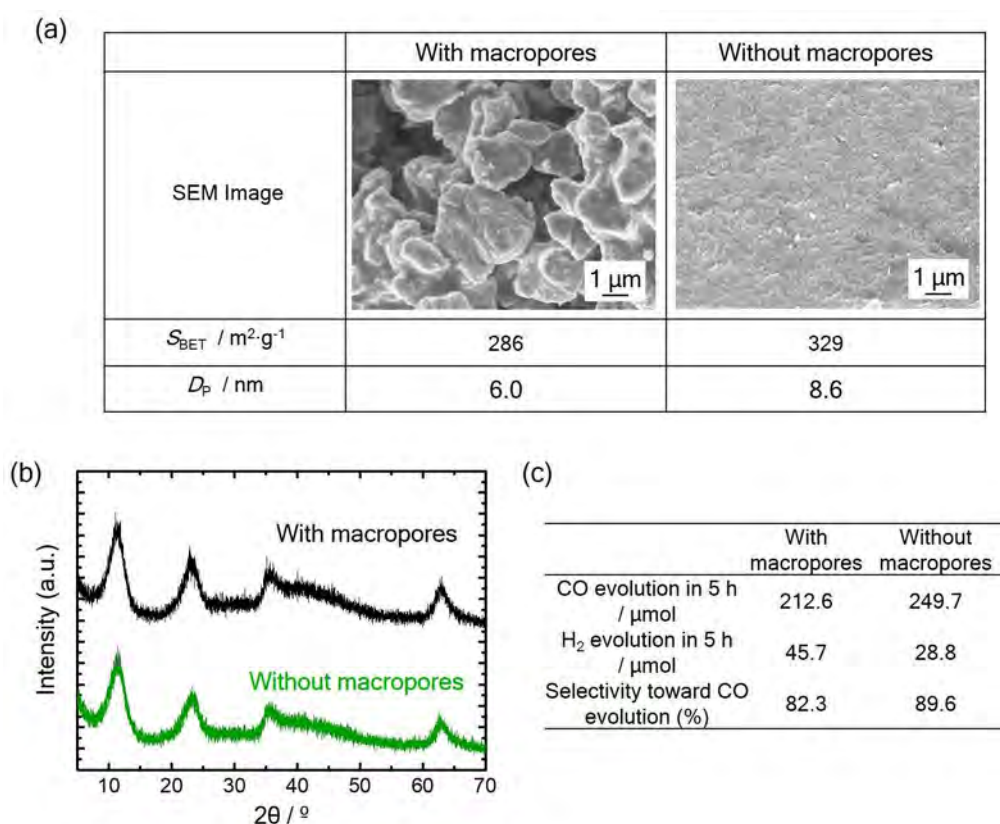
Figure S5. (a) Pore characteristics and (b) XRD patterns of NLDH-05 with and without macroporous structure. The LDH sample with macropores were prepared in the presence of 0.03 g of poly(ethylene oxide) (PEO). The amounts of CO gas evolved after 5 h light illumination were 212.6 and 249.7 μmol for the catalysts with and without macropores, respectively. The results suggest that the introduction of macroporosity does not have any considerable effect on the catalytic activity; CO_2 molecules are small enough to diffuse through mesopores to catalytically active sites on the solid surface, even without the introduction of macropores.
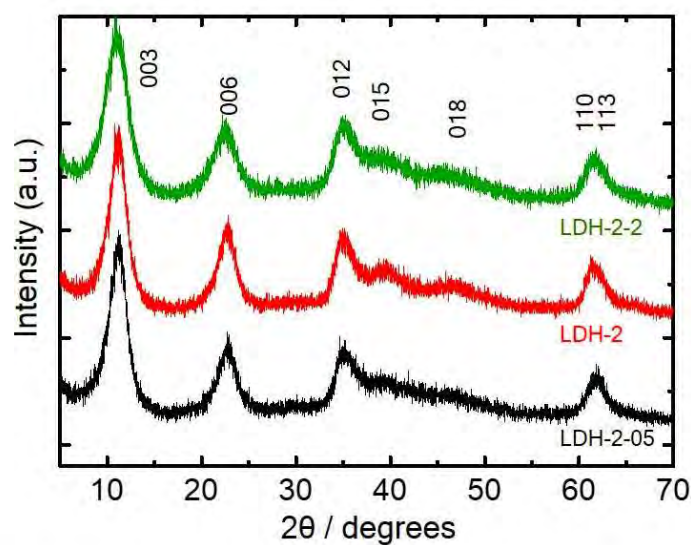
ID	Structural features		Catalytic properties		
	S_{BET} /m$^2\cdot$g^{-1}	(003) Crystallite size /nm	CO evolution in 5 h / μmol	H$_2$ evolution in 5 h / μmol	Selectivity toward CO evolution (%)
NLDH-2-2	255	2.97	176.41	48.63	78.4
NLDH-2	238	3.61	220.84	43.57	83.5
NLDH-2-05	93	3.71	246.01	43.73	84.9

Figure S6. Relationship between BET specific surface area and catalytic properties of nano LDH. The samples possess a comparable crystallinity and a chemical composition. The relatively small S_{BET} for NLDH-2-05 is due to large shrinkage of hydroxide gel during drying to form a denser xerogel structure. Interestingly, the amount and the selectivity of CO evolution do not depend on the surface area. These samples were prepared from the precursory solutions listed in **Table S2**.
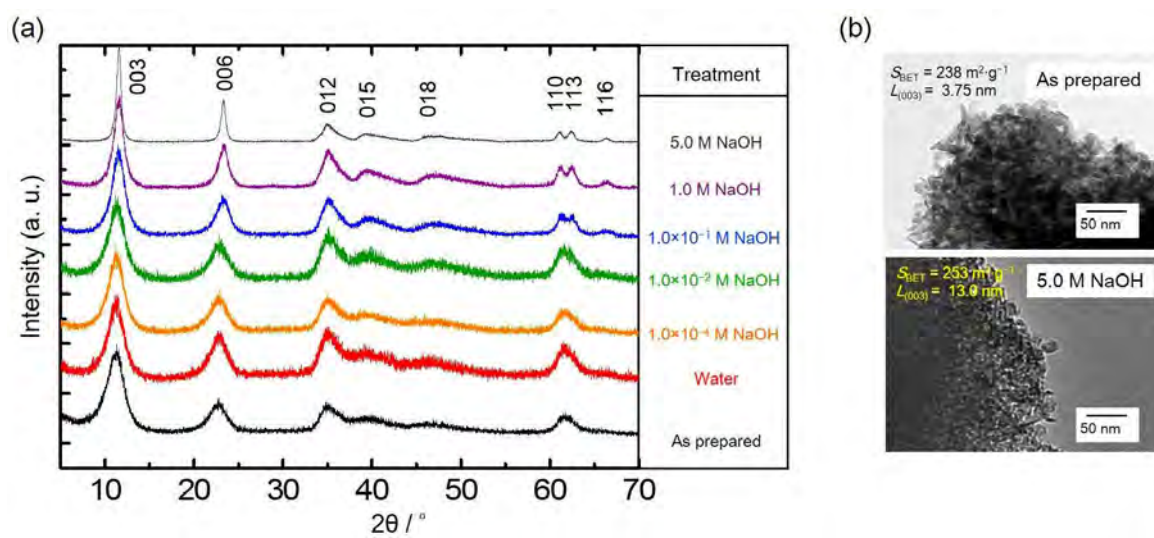
Figure S7. (a) XRD patterns and (b) TEM images of NLDH-2 after aging with NaOH solutions of various concentrations for 48 h.
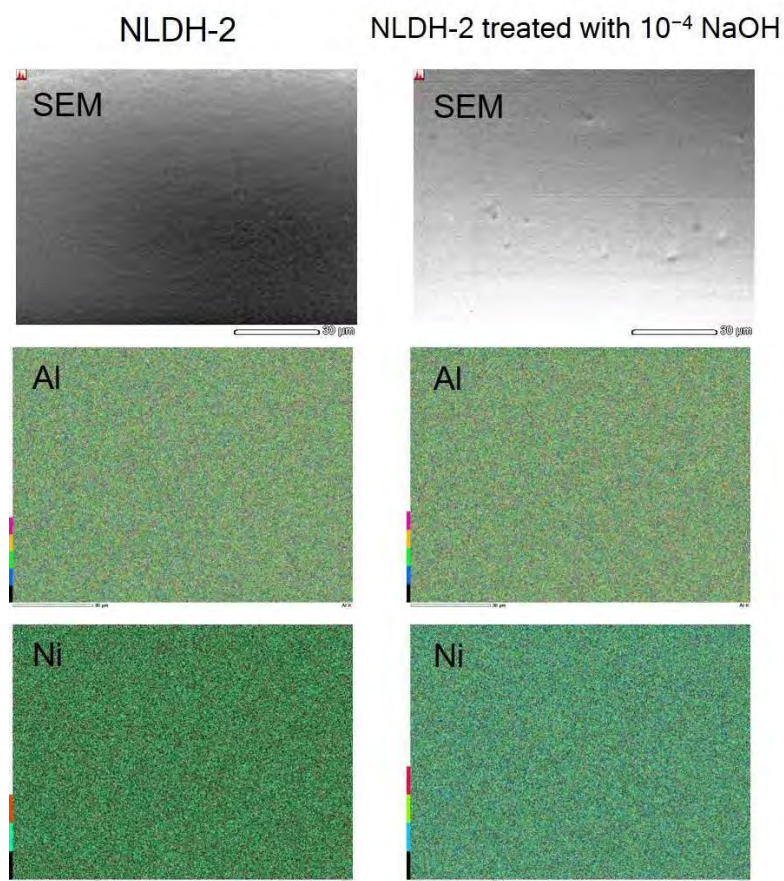
Figure S8. Elemental mappings of NLDH-2 before and after aging in 10^{-4} M NaOH. Both photocatalysts show homogeneous distribution of constituent cationic species (Ni(II) and Al(III)). A scanning electron microscope with an energy-dispersive X-ray spectrometer (SEM-EDS, JSM-6060S, JEOL) was used for the analysis.
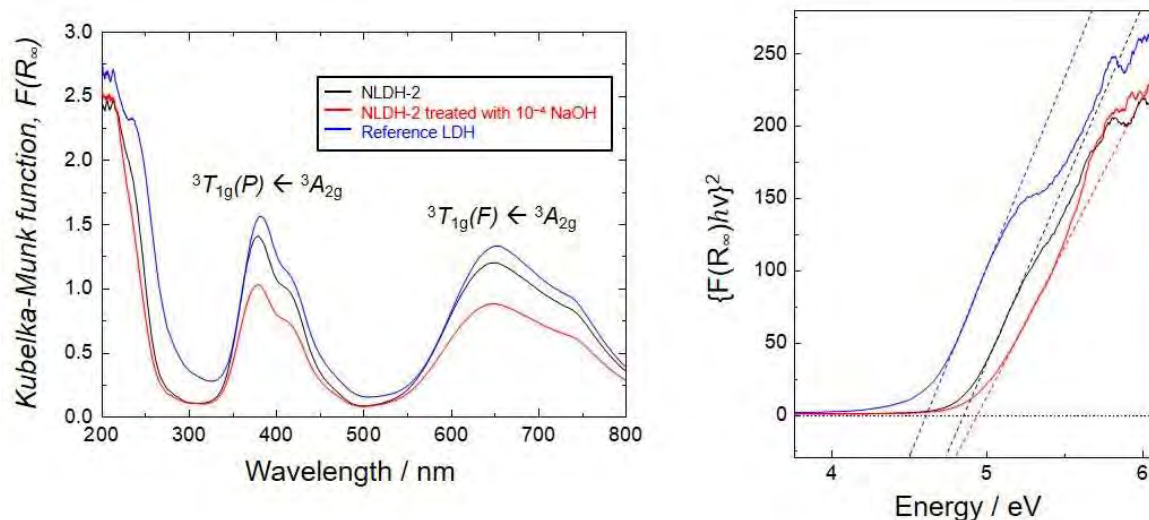
	NLDH-2	Reference LDH	NLDH-2 treated with 10^{-4} M NaOH
E_g /eV	4.9	4.6	5.0
CO_2 evolved /µmol	250	36	17

Figure S9. Summary of the results of UV-Vis spectroscopy on LDH samples, reference LDH, NLDH-2, and NLDH-2 treated with 10^{-4} NaOH. The values of E_g are good agreement with the ones for LDHs in the previous report.[4] The potential of photo-generated electron of standard LDH is reported to be high enough to reduce CO_2 into CO, which presents a clear difference with oxides, such as TiO_2 which are known to be inactive towards the photocatalytic reduction of CO_2.[5]

References

1. S. Iguchi, K. Teramura, S. Hosokawa and T. Tanaka, *PCCP*, 2015, **17**, 17995-18003.

2. S. Iguchi, K. Teramura, S. Hosokawa and T. Tanaka, *Catal. Today*, 2015, **251**, 140-144.

3. Y. Tokudome, *J. Ceram. Soc. Jpn.*, 2017, **125**, 597-602.

4. S. Iguchi, S. Kikkawa, K. Teramura, S. Hosokawa and T. Tanaka, *PCCP*, 2016, **18**, 13811-13819.

5. S. Navalón, A. Dhakshinamoorthy, M. Álvaro and H. Garcia, *ChemSusChem*, 2013, **6**, 562-577.